

8-30-2011

# Using vibration-based monitoring to detect mass changes in satellites

Breck Vernon

Follow this and additional works at: [https://digitalrepository.unm.edu/ce\\_etds](https://digitalrepository.unm.edu/ce_etds)

---

## Recommended Citation

Vernon, Breck. "Using vibration-based monitoring to detect mass changes in satellites." (2011). [https://digitalrepository.unm.edu/ce\\_etds/53](https://digitalrepository.unm.edu/ce_etds/53)

This Thesis is brought to you for free and open access by the Engineering ETDs at UNM Digital Repository. It has been accepted for inclusion in Civil Engineering ETDs by an authorized administrator of UNM Digital Repository. For more information, please contact [disc@unm.edu](mailto:disc@unm.edu).

Breck Vernon

*Candidate*

Civil Engineering

*Department*

This thesis is approved, and it is acceptable in quality and form for publication on microfilm:

*Approved by the thesis Committee:*

Dr. Arup K. Maji



, Chairperson

Dr. Mahmoud Reda Taha



Dr. Percy Ng



Accepted:

*Dean, Graduate School*

*Date*

**USING VIBRATION-BASED MONITORING  
TO DETECT MASS CHANGES IN SATELLITES**

**BY**

**BRECK ALAN VERNON**

B.S. Construction Engineering, University of New Mexico, 2008

THESIS

Submitted in Partial Fulfillment of the  
Requirements for the Degree of

**Masters of Science  
Civil Engineering**

The University of New Mexico  
Albuquerque, New Mexico

**July, 2011**

## **DEDICATION**

Dedicated to my wife, Lindsay, who has supported me throughout this long process. It has been stressful and frustrating at times, but her unwavering dedication to keeping me focused and determined has aided me in the completion.

## **ACKNOWLEDGEMENTS**

First and foremost, I would like to acknowledge my wife and family for their constant support and dedication to making sure that I succeed in my endeavors. They have supported me both financially and professionally throughout this process and they deserve a lot of credit for it.

Second, I would like to acknowledge my advisor, Dr. Arup Maji. I would like to thank him for his willingness to invite me into a program that I had little experience with and helping me all along the way to make sure that I was able to succeed.

Lastly, I would like to acknowledge the Air Force Research Laboratory Space Vehicles Directorate for their assistance throughout this process. Access to the resources in the labs and the help from various personnel were pivotal to my successful completion.

**USING VIBRATION-BASED MONITORING  
TO DETECT MASS CHANGES IN SATELLITES**

**BY**

**BRECK ALAN VERNON**

**ABSTRACT OF THESIS**

Submitted in Partial Fulfillment of the  
Requirements for the Degree of

**Masters of Science  
Civil Engineering**

The University of New Mexico  
Albuquerque, New Mexico

**July, 2011**

**USING VIBRATION-BASED MONITORING  
TO DETECT MASS CHANGES IN SATELLITES**

**By:**

**Breck Alan Vernon**

B.S., Construction Engineering, University of New Mexico, 2008

M.S., Civil Engineering, University of New Mexico, 2011

**ABSTRACT**

Vibration-based structural health monitoring could be a useful form of determining the health and safety of space structures. A particular concern is the possibility of a foreign object that attaches itself to a satellite in orbit for adverse reasons. A frequency response analysis was used to determine the changes in mass and moment of inertia of the space structure based on a change in the natural frequencies of the structure or components of the structure. Feasibility studies were first conducted on a 7 in x 19 in aluminum plate with various boundary conditions, which was impacted with a mallet and the frequency response was determined. The frequency response for the blank plate was used as the basis for detection of the addition, and possibly the location, of added masses on the plate. Statistical variation of the data was determined

to allow variations of frequency due to added mass and thermal changes to be evaluated. Effect on damping was also investigated. The test results were compared to both analytical solutions and finite element models created in SAP2000. The testing was subsequently expanded to aluminum alloy satellite panels and a mock satellite with dummy payloads to determine the thresholds of detectability.

## TABLE OF CONTENTS

LIST OF FIGURES .....	x
LIST OF TABLES .....	xii
CHAPTER 1 - INTRODUCTION .....	1
History .....	2
Literature Survey .....	3
Approach .....	6
CHAPTER 2 – EXPERIMENTAL PROCEDURES .....	8
Experimental Technique .....	8
Experimental Equipment .....	12
CHAPTER 3 – ANALYSIS AND BENCH-TOP EXPERIMENTS .....	12
Analytical Solutions .....	12
Numerical Models and Analyses .....	15
Discussion .....	18
Cantilever Plate .....	19
Pseudo-Simply Supported Plate .....	20
Fixed-Fixed Plate .....	23
Temperature Effects .....	27
Statistical Analysis .....	29
Analysis of Aluminum Test Plate Results .....	30
CHAPTER 4 – SATELLITE TESTING .....	35
PnP 2 Iso-Grid Satellite Panel .....	35
Mock Satellite .....	40

CHAPTER 5 – CONCLUSIONS.....	45
Conclusion.....	45
Recommendations for Future Work .....	47
APPENDIX A – Material Properties for Aluminum Test Plate .....	49
APPENDIX B – Fundamental Frequencies for Various Satellites.....	50
REFERENCES .....	51

## LIST OF FIGURES

Figure 2.1: Overall Plan View of Aluminum Test Panel Setup.....	8
Figure 2.2: Profile View of Aluminum Test Panel Setup with Fixed-Fixed Boundary Condition.....	9
Figure 2.3: Profile View of Aluminum Test Panel Setup with Simply Supported Boundary Condition.....	9
Figure 2.4: Profile View of Aluminum Test Panel Setup with Cantilever Boundary Condition.....	10
Figure 2.5: Photo of Aluminum Test Plate Setup.....	11
Figure 3.1: Fixed-Fixed SAP2000 Model (Mode 1 Response) .....	15
Figure 3.2: Fixed-Fixed SAP2000 Model (Mode 2 Response) .....	16
Figure 3.3: Fixed-Fixed SAP2000 Model (Mode 3 Response) .....	16
Figure 3.4: Impact Response of the Pseudo Simply Supported Plate.....	22
Figure 3.5: Frequency Spectrum of the Pseudo Simply Supported Plate (Linear Scale) .....	22
Figure 3.6: Zoomed Section of the Dominant Frequency on the Psuedo Simply Supported Plate.....	22
Figure 3.7: Impact Response of the Fixed-Fixed Plate.....	26
Figure 3.8: Frequency Spectrum of the Fixed-Fixed Plate (Linear Scale) .....	26
Figure 3.9: Zoomed Section of the Dominant Frequency on the Fixed-Fixed Plate .....	26
Figure 3.10: Frequency Values for 10 Days of Testing.....	28
Figure 3.11: Frequency Ranges to One Standard Deviation for Each Mass .....	31
Figure 3.12: Frequency Ranges to One Standard Deviation for Each Mass Compared to Blank Plate Temperature Cycles.....	33

Figure 4.1: PnP 2 Test Panel Setup.....	36
Figure 4.2: Photo of PnP 2 Setup Showing Accelerometer Location.....	37
Figure 4.3: Photo Showing How the Setup was Clamped to the Table.....	37
Figure 4.4: Photo of PnP 2 Setup Showing a Mass Bolted to the Plate.....	38
Figure 4.5: Frequency Ranges to One Standard Deviation for PnP 2 Testing .....	39
Figure 4.6: Frequency Ranges to One Standard Deviation for PnP 2 Testing from 0 - 246.5 grams.....	40
Figure 4.7: Diagram of Mock Satellite Test Setup .....	41
Figure 4.8: Photo of Mock Satellite Test Setup with Mass Attached.....	42
Figure 4.9: Photo Showing Connection Between Panels on Mock Satellite .....	42
Figure 4.10: Frequency Range to One Standard Deviation for Mock Satellite Testing.....	43

## LIST OF TABLES

Table 3.1: Analytical Results for the First Three Modes for Each Boundary Condition .....	14
Table 3.2: SAP2000 Results for Each Boundary Condition.....	17
Table 3.3: SAP2000 Results for Adding Masses to Fixed-Fixed Plate .....	18
Table 3.4: Average Natural Frequencies of Aluminum Test Panel at Locations 1 & 2 .....	23
Table 3.5: Average Natural Frequencies of Aluminum Test Panel at Location 3 .....	24
Table 3.6: Statistical Results of Testing at Location 1 .....	31
Table 3.7: Test Results for Aluminum Plate with Added Masses .....	32
Table 4.1: Statistical Results of Testing on PnP 2 .....	39
Table 4.2: Statistical Results for Mock Satellite Testing.....	42

## Chapter 1

### INTRODUCTION

A structure, when excited, will dissipate energy by vibrating at its natural resonant frequencies. Elements of a structure will have different vibration frequencies and corresponding modes that can vary based on the material, the boundary conditions, whether or not that material is isotropic or homogeneous, etc. Knowing these natural vibration frequencies and understanding how they change in a structure is an important part of Structural Health Monitoring (SHM). Vibration-based SHM provides useful information as to the health and safety of a structure. Using frequency response analysis as a method of determining changes in the mass or moment of inertia of a space structure is a complex undertaking due to the added circumstances of operating in the remote and unfamiliar environment of space. Exciting a model structure and measuring the resulting resonant frequencies of that structure is relatively simple to do. Analyzing the results and using them to understand how a full-scale structure will behave is a much more difficult task.

This research investigates the ability to detect an added mass to a satellite or other similar space structure by analyzing the impact response under different scenarios and comparing it to a previous baseline response. The idea is to constantly monitor the dynamic characteristics of a structure such as the modal frequencies, modal shapes and damping ratios and determine, based on changes in these characteristics, the presence of an additional mass or loss of existing mass on the structure. Additionally, a finite

element model was created matching that of the experiment to compare and determine the reliability of computer modeling as a way of determining the behavior of a specific structure and the effect of adding a mass.

## **History**

Vibration-based SHM has been performed for many years on many different types of structures. A majority of the testing that has been done has investigated the ability to detect damage on a structure, with most of those structures being bridges. This testing has proven to be accurate and reliable and has led to the development of many different types of methods for vibration-based structural monitoring. Some of the more popular methods involve frequency response analysis, similar to what was used in this research. Additionally, real-time monitoring of the stresses and strains experienced by a structure in critical areas is another common SHM method.

There also exist many different types of data acquisition sensors that gather the response data from the structure but a continuing problem is identifying the most effective and realistic way to excite the structure. There are basically two different excitation sources for structures; artificial excitation such as mass drops, a vehicle accelerating or braking on a bridge or a large mass shaker; and, natural excitation such as wind, waves or earthquakes. These methods have been used as a form of excitation on earthbound structures; however, excitation gets slightly more complicated when a structure is in orbit. Possible solutions for excitation of a space structure will be discussed later on. Further complicating matters is the effect of temperature on the

vibration of materials. Temperature effects on vibration-based damage detection for a bridge are explored by Peteers et al. (2001) where they determine a way to filter out the temperature effects from damage detection. Determining the temperature effects of a structure in space is a much more complex process given the range of temperatures seen outside of earth's atmosphere.

### **Literature Survey**

There are many different methods and types of equipment available for vibration-based SHM. However, a majority of the research that has been done has been for damage detection on a structure, with a majority of the structures being earthbound structures. SHM of space structures is certainly nothing new but very little, if any, previous investigation has occurred to detect mass changes on satellites by means of vibration-based analysis.

The overall success of SHM has been enhanced due to the use of more complex methods such as analyzing the frequency response by way of the frequency response function (FRF) curvature method investigated by Sampaio et al. (2003) for damage detection. Sampaio et al. (2003) witnessed that analyzing mode shapes as a way of damage detection proved to be unreliable when the damage was located close to a node and showed that FRF's overcame this problem. Also investigating frequency response was Moreno et al. (2005), who used a laser vibrometer to measure the response of a plate in order to avoid any structural changes caused by accelerometer loading. Damage location and severity on a bookshelf structure was successful

determined using a systematic comparison and correlation between two sets of vibration data was investigated also as a way to circumvent errors seen by mode shape analysis by Zang et al. (2007). This work was expanded on further by Shi et al. (2000) by using incomplete mode shapes for detection and localization. The present research incorporates portions of some of the methods previously used by analyzing the structure through a comparison of frequency responses obtained under different conditions, a loaded state versus a base-line unloaded state.

Fu-Kuo Chang and his colleagues (Wu et. al., 2009, Qing et. Al., 2007) have done extensive research on structural health monitoring including composite materials. Their work provides an overview of sensor technology and data synthesis relevant to interrogation of structures. However, their research did not pertain to the effect of mass changes on structures or components.

Extensive research has been done in regards to modal analysis of plates and beams. Specifically, the Shock Response Spectrum was measured in a plate that was subjected to impulse loading (Botta and Cerri, 2007). In addition, Adams et al. (1978) found that, with fiber-reinforced plastics, a state of damage could be detected by a reduction in stiffness and an increase in damping; this was true whether the damage was localized, as in a crack, or distributed through the bulk of the specimen, in the form of many microcracks.

In addition to an overall assessment of damage detection on a structure, many researchers have focused on specific parts of a structure where damage could occur (i.e.

bolts, joints, etc.). Lee and Shin (2002) investigated using the frequency-domain method as a way of damage detection in a cantilever beam using the frequency response equations. Ritumrongkul et al. (2003, 2004) looked at the structural health of a bolted joint using a Piezoceramic (PZT) as both an actuator and a sensor.

Complicating the whole basis of detecting added masses on a structure by means of vibration analysis is determining the exact cause of the frequency change. The presence of damage on a structure such as a crack could potentially have the same effect as an added mass as both would be expected to change the natural frequencies and mode shapes. The damage detection by means of frequency response functions used by Zang et al. (2007) and Sampaio et al. (2003) have determined that the changes in the Frequency Response Functions are fairly reliable when it comes to damage detection. Further attention would need to be paid to determining if there is a separation in the frequency response of a damaged structure versus a structure with an added mass.

Structural Health Monitoring of civil infrastructure typically involves passive monitoring due to the difficulties in exciting large structures. The research reported here involves active SHM in the context that vibration is induced by an impact. Another major difference is that in large structures the effect of temperature is delayed or reduced due to the thermal mass of the structure, while smaller test equipment and more susceptible to thermal effects.

## **Approach**

A primary concern driving this research is the potential of a mass of some size and shape attaching to a satellite while in orbit. Therefore, the goal is to see if it is possible to detect a change in the mass of an aluminum plate or a mock satellite by analyzing its natural vibration frequencies and comparing it to the frequency obtained under a base-line (no mass) condition. The first vibration testing began on a 7 in. x 19 in. 6061-T6 aluminum plate subject to three different boundary conditions: cantilever, pseudo-simply supported and fixed-fixed. Testing the three boundary conditions allowed for verification of the experimental instrumentation and results prior to testing satellite panels and a large scaled mock satellite. The experimental results were compared to exact analytical solutions as well as a finite element model (FEM) for the natural vibration frequency of an aluminum plate to validate the accuracy.

Using just the fixed-fixed boundary condition on the aluminum plate, varying masses were added to the plate and the resulting natural vibration frequencies of the plate were measured. Considering that the mass of an object is used in the calculation of its natural resonant frequencies, it was expected that the addition of mass would change an objects fundamental frequencies. The goal was to see what range of masses were detectable on the plate. Although not initially part of the plan, the effect of temperature fluctuations complicated matters and was investigated. Again, results were compared to FEM's to test the reliability of a computer program to accurately model this type of testing.

Finally, this same testing was expanded to individual satellite panels as well as a large scale mock satellite at the Air Force Research Laboratory Space Vehicles Directorate. Two iso-grid aluminum alloy satellite panels were attached at a 90 degree angle forming a cantilever, upon which masses were added and resulting frequencies were measured to determine the smallest detectable mass on the panel. Secondly, six iso-grid panels were connected to form a mock satellite upon which the same vibration testing was performed to determine the smallest detectable mass on a large scale satellite structure. The testing on the satellite and its components was done inside of a lab where the environment is controlled, thus temperature did not have an impact.

## Chapter 2

### EXPERIMENTAL PROCEDURES

#### Experimental Technique

An accelerometer was attached to a 7 in. x 19 in. aluminum plate (approximate weight of 740 grams) in order to measure vibrations in the plate. The use of a single sensor limits the ability to detect and distinguish the contribution of different modes and the associated energy, which were beyond the scope of this research. The plate is bolted down with two rows of four bolts (total 8) at each end to a sturdy base giving a 15" span between bolts (see figure 2.1).

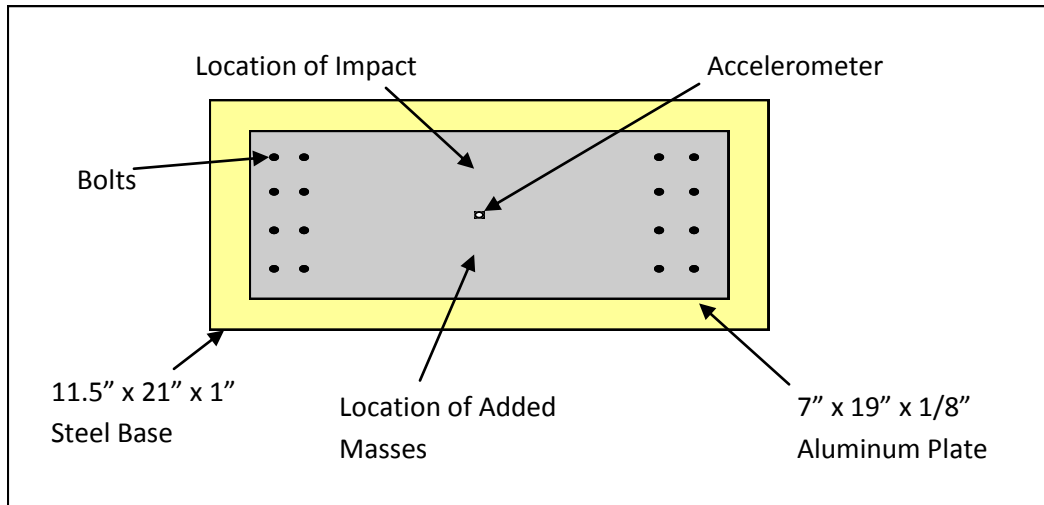


Figure 2.1: Overall Plan View of Aluminum Test Panel Setup

With the setup depicted in Figure 2.1, three different boundary condition cases were tested:

- 1) All bolts tightened down to simulate a fixed-fixed condition (Figure 2.2).

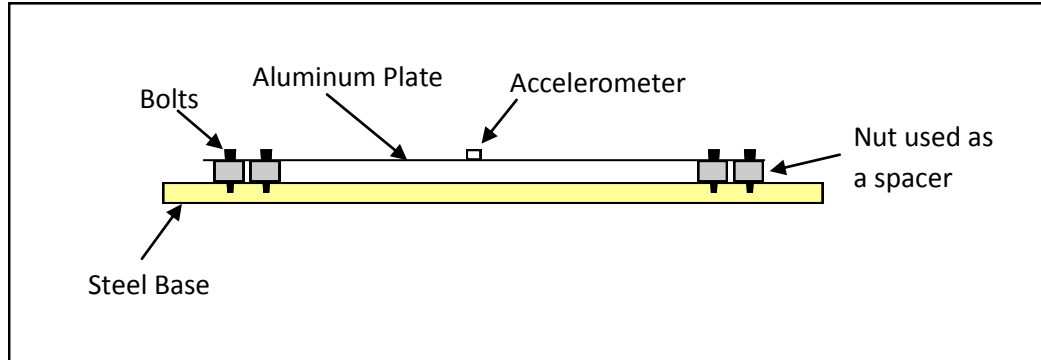


Figure 2.2: Profile View of Aluminum Test Panel Setup with Fixed-Fixed Boundary Condition

- 2) One row of bolts removed and each of the remaining bolts were loosened allowing for slight rotation but no translation at both ends resulting in a pseudo simply-supported case (Figure 2.3). A more appropriate means of achieving simply supported condition might have been to incorporate rollers between the plates to allow controlled rotation.

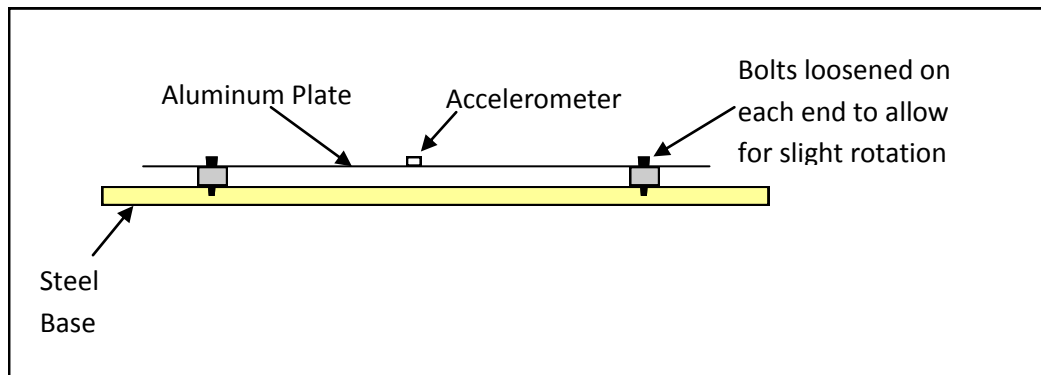


Figure 2.3: Profile View of Aluminum Test Panel Setup with Pseudo Simply Supported Boundary Condition

- 3) One set of bolts was completely removed while the other side is tightened to simulate a cantilever case (Figure 2.4).

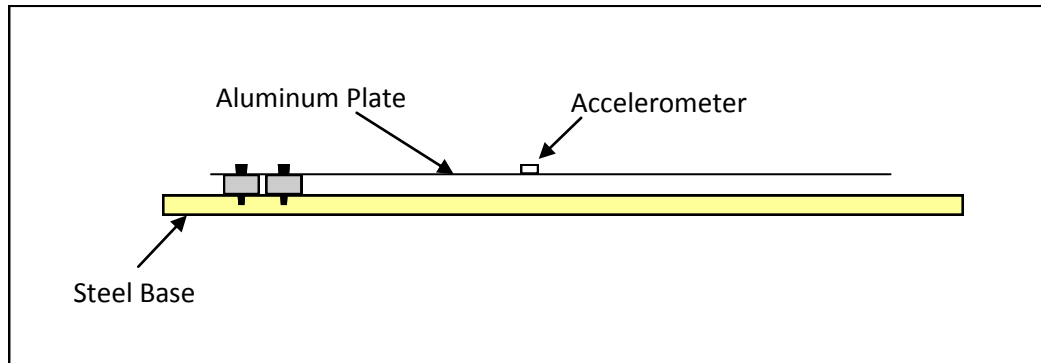


Figure 2.4: Profile View of Aluminum Test Panel Setup with Cantilever Boundary Condition

The accelerometer was left attached to the center of the plate in all three cases. The plate was then impacted lightly with a small rubber mallet and the accelerometer gathered the data from the response. The gap between the aluminum plate and the steel base was large enough (approximately 1/4 inch) so as to not allow the two plates to touch following the impact. Data from the accelerometer is analyzed using Labview where a Fast-Fourier Transform is performed to find the frequency content. The exact analytical solutions for the natural vibration frequency of a plate or a beam are known and were calculated for this plate to compare to experimental results.

The three boundary conditions were tested, recorded and used to compare the experimental data to analytical solutions and the finite element models to confirm the accuracy of the system. A majority of the testing was done on the fixed-fixed plate due to it being the boundary condition most closely resembling what is experienced by a panel as part of a satellite in space. Even though the satellite is in an environment with

little gravity and not attached to anything, each panel is itself fixed on all edges to the other panels.

The fixed-fixed and cantilever cases were simple to create but a simply supported case was more difficult given the attachments used, therefore this case will be referred to as the pseudo-simply supported boundary condition. Removing the outer row of bolts and loosening the interior row to allow for rotation proved acceptable but not exact, based on comparisons of experimental data and analytical data presented in Chapter 3. The ideal simply supported case would have rollers that allow for rotation on both ends and translation on one end. Using rollers on a plate of this size and weight would have been problematic upon impact. The accuracy of the test plate setup was compared with results from the experiments, SAP2000 -based finite element models and analytical solutions, discussed in Chapter 3. Figure 2.5 below is a photo of the actual aluminum test plate setup.



Figure 2.5: Photo of Aluminum Test Plate Setup

## **Experimental Equipment**

A 7 in. x 19 in. 6061-T6 aluminum plate with a thickness of 1/8 inch was used as a feasibility study. The aluminum plate is bolted to a heavy duty steel plate that acts as a stable base for the vibration testing, leaving a gap of approximately 1/4 inch between the aluminum plate and the steel plate. An ICP Accelerometer from PCB Piezotronics, Inc. in Depew, New York is attached to the plate using a basic adhesive. The model 352C41 accelerometer has a sensitivity of 10 mV/g and a frequency range from 1.0 to 9000 Hz. The data from the accelerometer was gathered by a NI USB-9234, 4-channel, 24-bit, DAQmx USB data acquisition device from National Instruments. The data acquisition device attaches to the laptop by means of a USB cable and a Labview program specifically written to analyze spectrum measurements provided the analyzed data showing vibration frequencies experienced by the impacted plate. The Labview program acquired 30k samples at a rate of 3 kHz each test run.

## Chapter 3

### ANALYSIS AND BENCH-TOP EXPERIMENTS

#### Analytical Solutions

Chopra (2007) provides the equations of the first three fundamental modes of natural vibration frequency of a cantilever, simply supported and fixed-fixed beam. The first mode vibration frequency for a cantilever beam is obtained by:

$$\omega = \frac{3.516}{L^2} \sqrt{\frac{EI}{m}} \quad (\text{Equation 3.1})$$

With the second and third modes equations being:

$$\omega = \frac{22.03}{L^2} \sqrt{\frac{EI}{m}} \quad (\text{Equation 3.2})$$

$$\omega = \frac{61.70}{L^2} \sqrt{\frac{EI}{m}} \quad (\text{Equation 3.3})$$

The analytical solution for the first order natural vibration frequency of the same beam if simply supported is given by Chopra (2007) as:

$$\omega = \frac{\pi^2}{L^2} \sqrt{\frac{EI}{m}} \quad (\text{Equation 3.4})$$

The second and third modes are given by:

$$\omega = \frac{4\pi^2}{L^2} \sqrt{\frac{EI}{m}} \quad (\text{Equation 3.5})$$

$$\omega = \frac{9\pi^2}{L^2} \sqrt{\frac{EI}{m}} \quad (\text{Equation 3.6})$$

The analytical solution for the first order natural vibration frequency for the same beam fixed at both ends is given by Chopra (2007) as:

$$\omega = \frac{22.37}{L^2} \sqrt{\frac{EI}{m}} \quad (\text{Equation 3.7})$$

The second and third modes are given by:

$$\omega = \frac{61.67}{L^2} \sqrt{\frac{EI}{m}} \quad (\text{Equation 3.8})$$

$$\omega = \frac{120.9}{L^2} \sqrt{\frac{EI}{m}} \quad (\text{Equation 3.9})$$

Using the equations given above, the following natural frequencies were calculated for the first three modes for each boundary condition.

**Table 3.1: Analytical Results for the First Three Modes of Each Boundary Condition**

Cantilever Plate (Hz)		Simply-Supported Plate (Hz)		Fixed-Fixed Plate (Hz)	
Mode 1		Mode 1		Mode 1	
$\omega$	13.89	$\omega$	50.09	$\omega$	113.53
Mode 2		Mode 2		Mode 2	
$\omega$	87.05	$\omega$	200.36	$\omega$	312.99
Mode 3		Mode 3		Mode 3	
$\omega$	243.80	$\omega$	450.82	$\omega$	613.60

## Numerical Models and Analyses

In an attempt to verify the validity of both the experimental results and the analytical calculations, a FEM of the plate was created in SAP2000. Another reason for creating the model in a computer program is to see if, for the purpose of expanding this work or for future work, the models could give accurate results and the process of conducting the tedious experiments could be avoided. An attempt was made to generate models for the iso-grid satellite panels but the complexity of those panels made creating them a very difficult process that time did not allow for. Therefore, finite element models were only created for the aluminum test plate setup. A model was created for each boundary condition that matched dimensions and material properties. For the fixed-fixed plate, different models were run similar to the experiments, adding masses and monitoring the change in natural frequency.

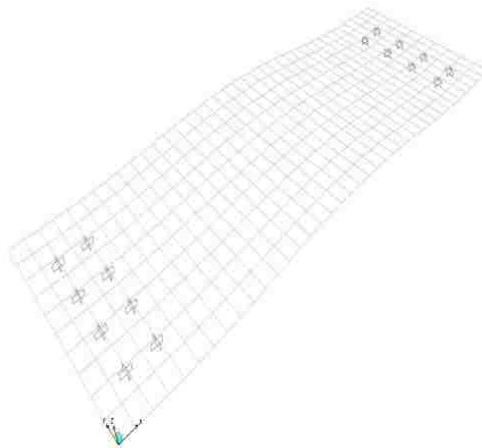


Figure 3.1: Fixed-Fixed SAP2000 Model (Mode 1 Response)

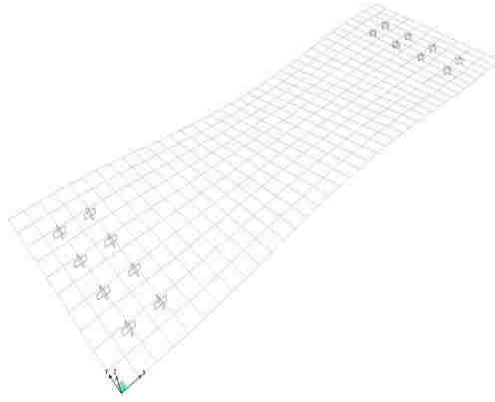


Figure 3.2: Fixed-Fixed SAP2000 Model (Mode 2 Response)

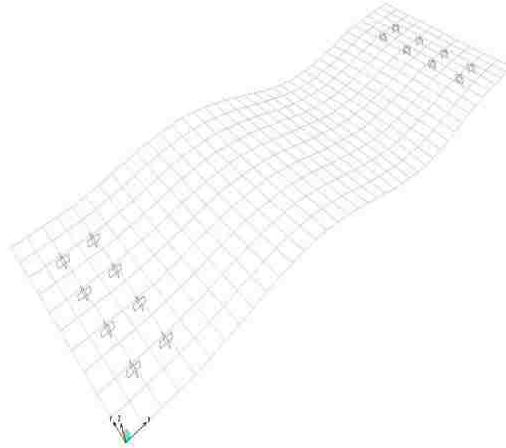


Figure 3.3: Fixed-Fixed SAP2000 Model (Mode 3 Response)

Table 3.2 below shows the first, second and third modes of natural vibration frequency results determined in SAP2000 for the cantilever, simply-supported and fixed-fixed plate.

Table 3.2: SAP2000 Results for Each Boundary Condition

Cantilever Plate (Hz)		Simply-Supported Plate (Hz)		Fixed-Fixed Plate (Hz)	
Mode 1		Mode 1		Mode 1	
$\omega$	13.98	$\omega$	49.70	$\omega$	112.79
Mode 2		Mode 2		Mode 2	
$\omega$	69.08	$\omega$	164.15	$\omega$	184.27
Mode 3		Mode 3		Mode 3	
$\omega$	87.09	$\omega$	191.40	$\omega$	309.43

To simulate the added masses in the experiments, masses were added to the computer model to determine the resulting frequencies. Table 3.3 below shows the frequencies obtained for the first three modes of the fixed-fixed plate when adding mass to it.

Table 3.3: SAP2000 Results for Adding Masses to Fixed-Fixed Plate

SAP2000 Results for Fixed-Fixed Plate with Mass		
Mass (g)	Mode	Frequency (Hz)
0	1	112.79
	2	184.27
	3	309.43
1	1	113.11
	2	184.27
	3	309.46
2	1	112.8
	2	184.24
	3	309.43
5	1	111.89
	2	184.15
	3	309.37
10	1	110.42
	2	184.01
	3	309.27
20	1	107.62
	2	183.75
	3	309.07
50	1	100.25
	2	183.03
	3	308.48
100	1	90.6
	2	182.02
	3	307.59

**Discussion**

Comparing Table 3.1 and 3.2, it can be seen that the frequencies obtained from the FEM analyses for the first mode of each boundary condition case are very similar to the analytical solutions (less than 1% difference). The fundamental frequencies were

also similar to that of the tests reported earlier (except for the simply-supported case for reasons discussed earlier). The results for the cantilever beam are almost identical and that of the fixed-end condition show just a slight difference in value that could be attributed to difficulty in attributing an exact length to a fixed-end condition created by two rows of bolts

The first modes from the FEM analyses (bending mode, Figure 3.1) shown in Table 3.3 are very similar to the test results reported in Table 3.6 later on in the chapter. The 2<sup>nd</sup> mode in the FEM analyses corresponds to a torsional mode (Figure 3.2) which was not considered in the analytical solutions. The results obtained for mode 3 (the second bending mode, Figure 3.3) with SAP2000 are very similar to the results calculated for the corresponding 2<sup>nd</sup> bending mode by the analytical solutions for each respective boundary condition.

Following are the experimental results obtained from the three different boundary conditions on the aluminum plate.

### **Cantilever Plate**

An attempt to replicate the effects on a cantilever beam was created by removing all 8 bolts at one end and tightening the 8 bolts at the opposite end. To avoid removing and re-attaching the accelerometer to the plate multiple times, the accelerometer remained attached in the center of the plate during the testing on the cantilever plate, where it was best located while measuring with the other two boundary condition cases. For the simply supported and fixed-fixed cases, having the

accelerometer in the middle of the plate (directly between the nodes) allowed for the most precise modal measurements, considering the center of the plate would experience the largest deflection. Although the center of the plate was the most ideal location for 1<sup>st</sup> mode response, it was the location of a node for the 2<sup>nd</sup> mode which resulted in little to no response. Therefore, only the fundamental frequency for the aluminum plate was analyzed. Given the large relative deflections of the cantilever plate, the centrally-located accelerometer still provided accurate vibration response data.

The free end of the plate was tapped with the rubber mallet and a natural vibration frequency was recorded. There were consistently three different frequencies that occurred: 13.8, 69, and 83 Hz. It became evident the frequency of 13.8 Hz corresponded to the first resonant mode, 69 Hz to the second mode and 83 Hz to the third mode. Comparison of this data to analytical and finite element modeling is discussed later herein..

### **Pseudo-Simply Supported Plate**

Using the bolts to attach the ends of the plate made it difficult to simulate the simply-supported boundary condition. One row of 4 bolts was removed on each end of the plate leaving a single row of 4 bolts. The bolts were loosened to a certain degree, such that a small rotation could occur. A simply-supported condition could not be accurately replicated because even though the bolts allowed for some rotation, they restricted all translation at both ends. It is my opinion this is the reason the results of

this condition were not as close to the analytical solution and the computer models as the cantilever and fixed conditions. The dominant first-mode frequency seen during the testing fell in the range of 60-80 Hz.

The frequencies measured during the testing of the simply supported plate were inconsistent. As one might expect, the tightness of the bolts would affect the stiffness of the plate and in this particular case, changing the tightness of the bolts resulted in a frequency variance of roughly 20 Hz. The following figures show how the experimental data was gathered for the response of an impacted simply-supported plate using Labview.

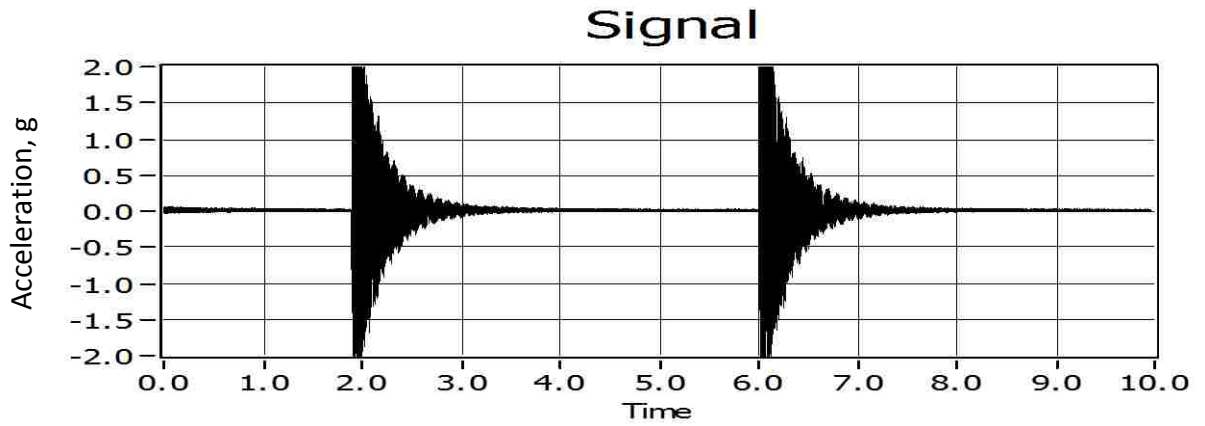


Figure 3.4: Impact Response of a Pseudo Simply Supported Plate

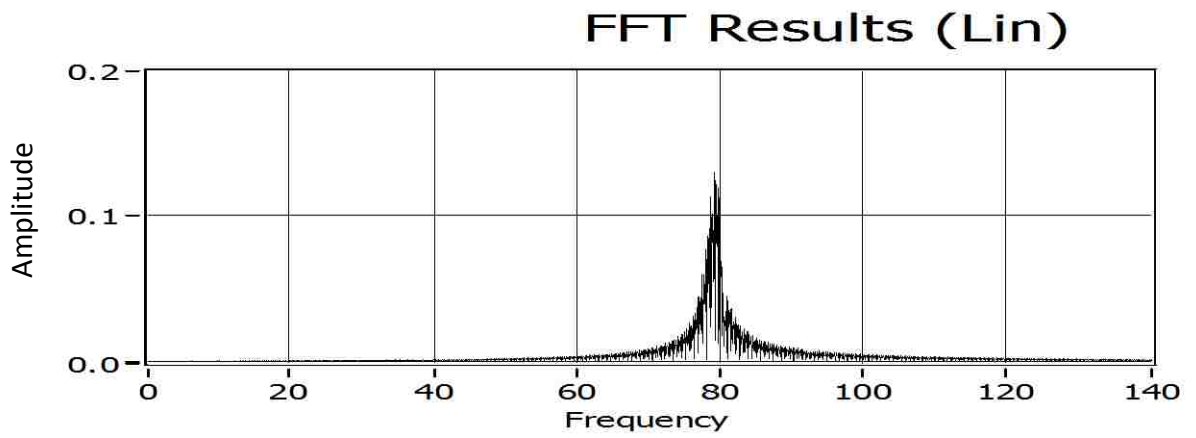


Figure 3.5: Frequency Spectrum for the Pseudo Simply Supported Plate (Linear Scale)

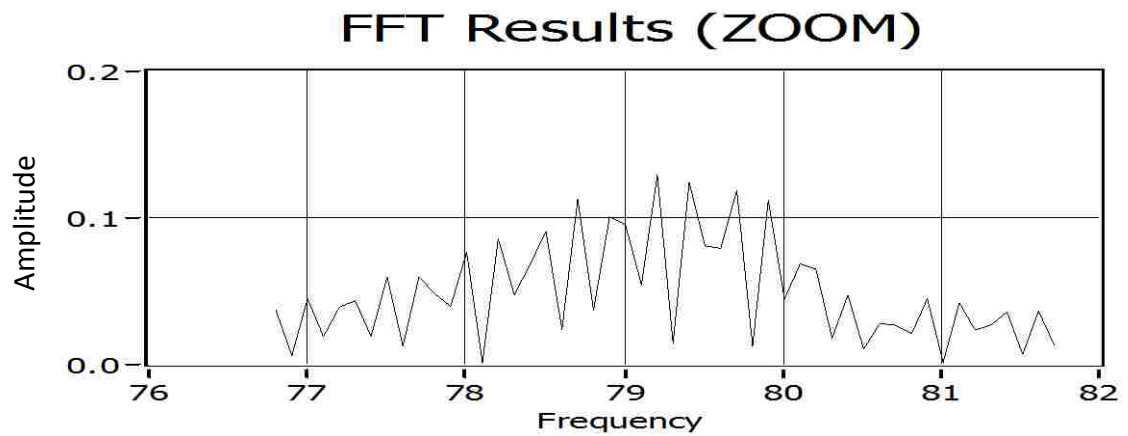


Figure 3.6: Zoomed Section of the Dominant Frequency on Pseudo Simply Supported Plate

## Fixed-Fixed Plate

The fixed-fixed plate boundary condition was used for a majority of the testing because it is believed to be the closest replication of the actual condition of a satellite panel. With the accelerometer still attached to the center of the plate and the excitation of the plate brought on by an impact at the center with a rubber mallet, a consistent dominant frequency was evident. A series of tests were done with the setup sitting on top of a desk in the structures lab at the University of New Mexico (location 1) and then the setup was moved to a desk top in an office (location 2) and then it was moved to the floor in the same office (location 3). Table 3.4 shows the results obtained when the setup was tested at locations 1 and 2 and table 3.5 shows the results obtained when the setup was at location 3.

**Table 3.4: Average Natural Frequencies of Aluminum Test Panel at Locations 1 & 2**

<b>Fixed-Fixed Aluminum Plate Natural Frequency Averages (location 1 &amp; 2)</b>		
Date	Average	Std. Dev.
2/5/2010	113.4	0.30
2/26/2010	113.7	0.06
3/14/2010	119.8	2.06
4/9/2010	113.9	1.87
4/10/2010	114.5	2.72
10/2/2010	111.5	0.60
10/3/2010	113.7	0.98
11/13/2010	116.1	0.04
11/26/2010	113.0	5.18
11/28/2010	116.1	1.73
12/3/2010	114.1	0.42
12/18/2010	117.6	0.34
12/19/2010	115.9	0.41
1/8/2011	118.0	0.91

**Table 3.5: Average Natural Frequencies of Aluminum Test Panel at Location 3**

<b>Fixed-Fixed Aluminum Plate Natural Frequency Averages (Location 3)</b>		
Date	Average	Std. Dev.
1/9/2011	124.1	2.92
1/10/2011	125.6	0.49
1/11/2011	126.0	0.40
1/12/2011	125.3	0.40
1/13/2011	124.8	0.49
1/15/2011	125.2	2.15
1/16/2011	125.7	2.03
1/17/2011	122.4	0.54
1/18/2011	121.9	0.29
1/19/2011	123.4	0.55
1/22/2011	122.9	1.49
1/30/2011	123.9	0.27

Some of the test results shown above represent an analysis where a full day of testing was performed and some represent an analysis of data for just a segment of time that testing could be performed on that day (i.e. 5 pm – 10 pm). The testing done for a full day is distinguishable by the higher standard deviations. Testing on the aluminum plate showed the natural frequency would tend to fall throughout the course of the day. The drop was not uniform but it was consistent and tended to follow a pattern. It was ultimately determined that temperature played a role in the fluctuation of the frequencies, however there was not a direct correlation due to the effect of the behaviors of both the aluminum test plate and the steel base plate under changing temperatures. A more detailed explanation of the temperature effects is discussed later in the chapter.

As seen in the difference in results from Table 3.4 to Table 3.5, there was a substantial difference in the natural frequencies obtained based on location of the test set-up in the laboratory. From the beginning of the testing it was believed that the steel base would provide a sturdy foundation and prevent vibration from transmitting through it, into the substrate and ultimately having an effect on the results. Moving the setup from the desk top to the floor was an attempt to test that theory.

Shown below is the response signal upon impact of the fixed-fixed plate followed by the results of a fast Fourier transform showing the dominant frequency followed by a zoomed in area of what's shown in Figure 3.8.

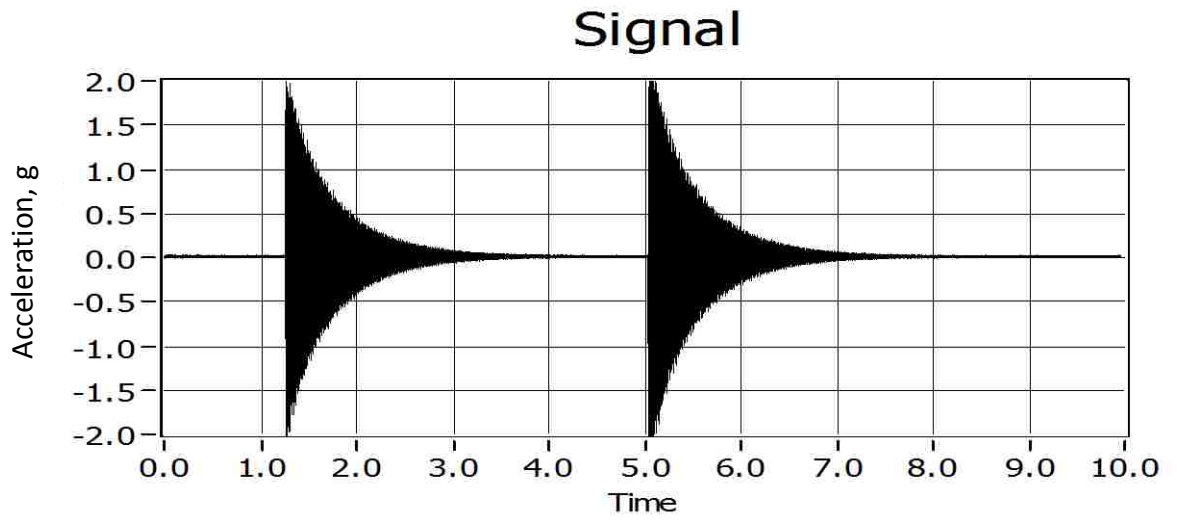


Figure 3.7: Impact Response of the Fixed-Fixed Plate

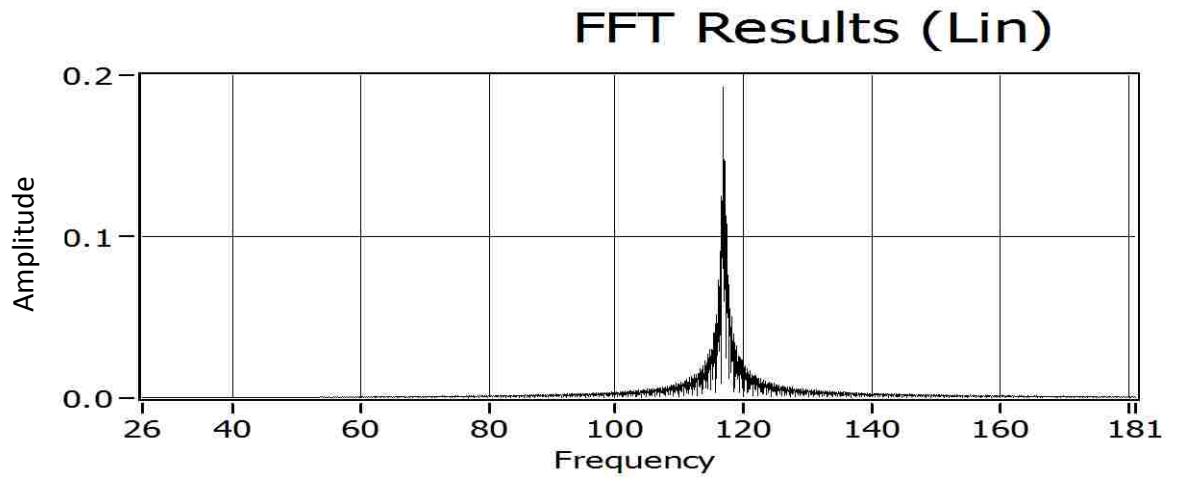


Figure 3.8: Frequency Spectrum of the Fixed-Fixed Plate (Linear Scale)

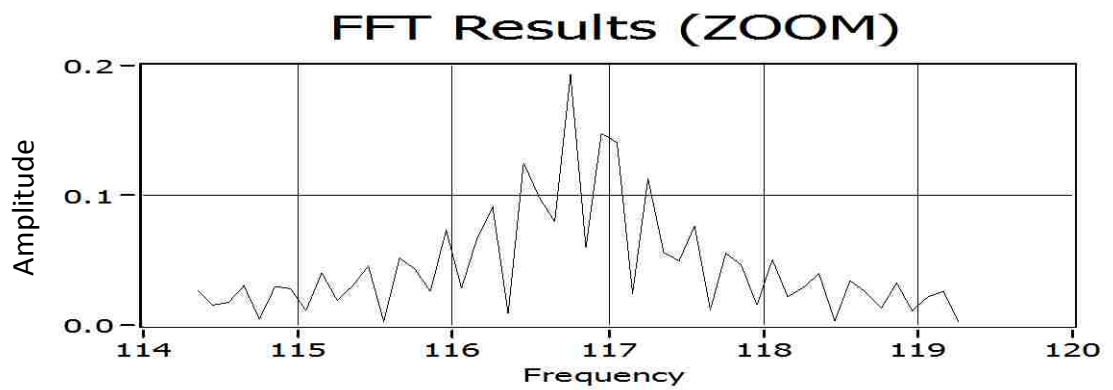


Figure 3.9: Zoomed Section of the Dominant Frequency on Fixed-Fixed Plate

## **Temperature Effects**

Throughout the testing of the aluminum plate, the natural vibration frequencies measured would change throughout the course of the day. The frequencies would start out high and gradually decline throughout the day and only begin rising during the night. See figure 3.10 for a graphical representation of this occurrence. Each time a full day of testing was performed, this same pattern was seen. As one would expect, the temperature of the plate would fluctuate throughout the course of the day, typically beginning low and then rising until mid-afternoon at which point it would usually plateau and hold constant for a period of time. Later in the evening the temperature would begin dropping and would continue into the night before cycling through the process again. The temperature of the aluminum plate would also follow this same pattern.

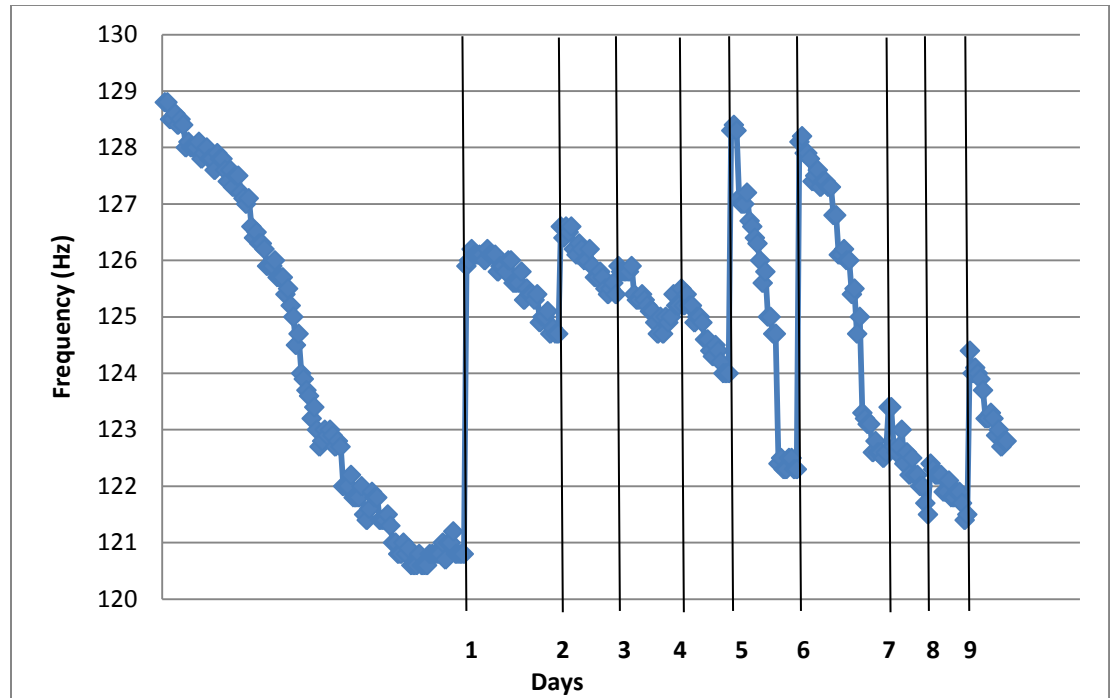


Figure 3.10: Frequency Values for 10 Days of Testing

An aluminum plate was used in this testing because aluminum alloy is the most commonly used metal for spacecraft structures (Larson and Wertz, 1999). The temperature effect can be attributed to the differential expansion of the aluminum, compared to that of the steel base, and the thermal inertial of the two metals with different size which leads to variation in the constraints on the plate.

A set of experiments were conducted to purposely change the temperature of the test set-up to verify this effect. Once the plate was heated up to about 80 degrees, vibration tests were conducted resulting in a natural frequency was much lower than prior to the plate being heated. The frequency drop was roughly 40 Hz with just a 5 degree increase in temperature. Tests were continued while the plate cooled back off

to room temperature and the frequency showed instant changes, rebounding consistently with the dropping temperature.

### **Statistical Analysis**

The criterion applied to determine if a mass is detectable on the plate was a 1-standard deviation separation from the base-line (no mass), hence, the mean obtained for a series of tests for a specific mass must fall outside of the range of one standard deviation of the mean of the plate with no mass on it. The range of mass added to the plate was from 1 to 100 grams early on in the testing and then a separate set of masses were obtained which allowed for testing from 0.8 to 100 grams, with smaller increments on the lower end. Determining a natural frequency for the plate with a 100 gram mass attached was fairly difficult as that much mass usually damped the vibration too quickly to determine a frequency. Given this, 100 grams was the upper limit of testing for the aluminum plate.

Additional insight as to the use of 1 standard deviation as the detectability criteria is as follows. The Hypothesis that is subject to statistical analysis is that 'the added mass results in a frequency shift'. In order to determine the confidence level for this hypothesis to be accepted, one needs to evaluate how the average frequency with the added mass  $\bar{x}$  differs from the average frequency of the baseline (no mass added),  $\mu$ . The standard deviation of the frequency data with no added mass is  $\sigma$ . To determine the confidence level it is necessary to evaluate the value of Z which relates the separation of the average frequencies to the standard deviation of the baseline:

$$Z = \frac{\overline{(\bar{x} - \mu)}}{\sigma/\sqrt{n}} \quad (\text{Equation 3.10})$$

Here  $\bar{x}$  is the average frequency with the added mass from  $n$  data points (tests). The value of  $Z$  provides the basis for confidence interval assuming a normal distribution of the data. Using a 1-standard deviation difference as the criteria for detectability implies that  $\bar{x} - \mu = \sigma$ , hence  $Z = \sqrt{n}$ . If  $n = 10$  (there were at least 10 data points with the added mass), then the probability of Type I error (determination of added mass when there is none) is only 0.08% (based on 1-tailed  $Z$  functions since added mass can only lead to a decrease in the frequency). A larger number of samples will further reduce the error while a smaller number of samples will increase the error and decrease the confidence interval (just 1 sample,  $n = 1$  will result in 16% probability of type 1 error).

### **Analysis of Aluminum Test Plate Results**

The testing done at locations 1 and 2 did not have any temperature recorded because it wasn't until later on that the realization was made that temperature might be a factor. Therefore, shown below (Table 3.6 and Figure 3.11) is one set of analyses from the results obtained from testing at location 1 without any temperature data present. The averages shown in Table 3.6 are a result of 30 or more tests at each listed mass. A second set of results obtained from location 3 with temperature data will be presented subsequently. Table 3.6 shows the averages and one standard deviation for the results obtained on testing of the blank plate and with a series of 7 different masses. Figure

3.11 shows the average of each different test and also shows the range determined by one standard deviation of the mean.

Table 3.6 Statistical Results of Testing at Location 1

Mass (g)	Average	Std. Dev.
0	113.8	1.20
1	113.2	1.84
2	113.1	1.94
5	111.7	0.24
10	111.5	1.95
20	109.2	2.01
50	102.6	0.41
100	86.0	7.60

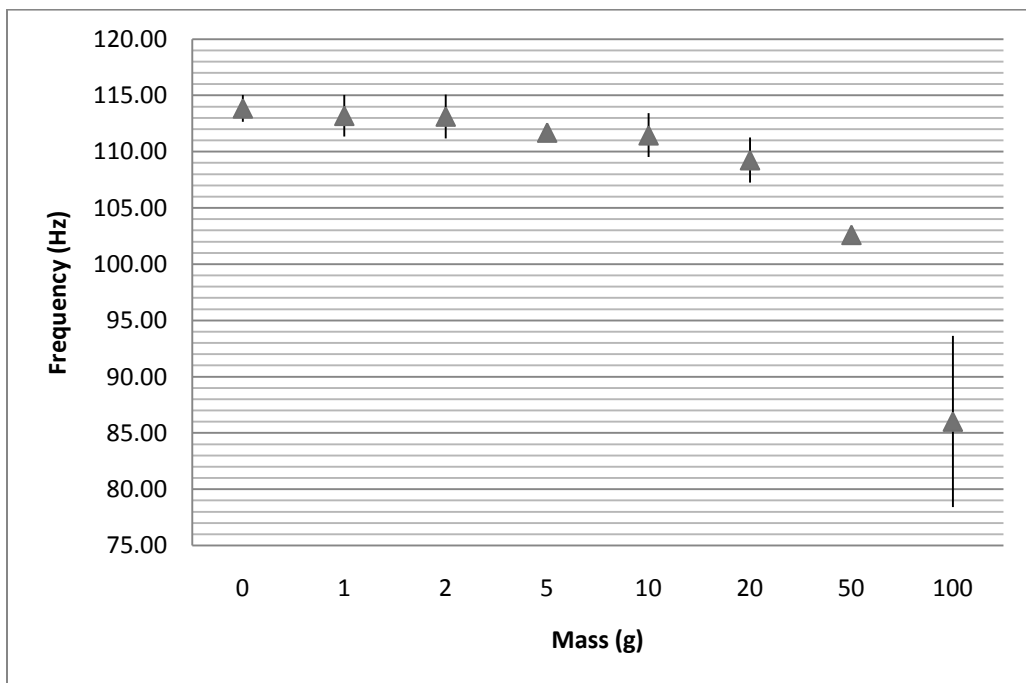


Figure 3.11: Frequency Ranges to One Standard Deviation for Each Mass

From figure 3.11, you can see that beginning at about 5 grams, the mean frequency has shifted sufficiently far as to determine that anything 5 grams or greater

would be detectable using the given evaluation criteria. Tests were also run with 200 and 500 gram masses on the plate but this much weight caused the vibration to dampen out too quickly and no distinguishable frequency could be recorded.

When it was observed that the frequencies were falling throughout the day, the temperature of the plate was recorded during testing to see if there was a thermal effect. In an attempt to troubleshoot the issues regarding the daily fall in frequencies, temperature data was only recorded when testing with no mass on the plate. Additionally, the frequency testing with mass was done during the periods of time when the plate temperature had stabilized in an attempt to remove the thermal effects from the frequency deviations. Table 3.6 and Figure 3.12 below show the results of testing with mass along with two different scenarios with no mass on the plate. Again, averages shown are a result of 30 or more tests at each listed description.

**Table 3.7: Test Results for Aluminum Plate with Added Masses**

Description	Average (Hz)	Standard Deviation	$\Delta T(^{\circ}F)$
All temperature recorded data (no mass)	124.3	2.16	16
7 days from the same time period (5pm -9pm) (no mass)	124.6	1.48	10
0.8 grams mass added to plate	123.8	0.06	-
1.4 grams of mass added to plate	123.6	0.09	-
3.6 grams of mass added to plate	123.3	0.48	-
7.4 grams of mass added to plate	123.0	0.20	-
14.8 grams of mass added to plate	121.5	0.78	-
18.4 grams of mass added to plate	120.6	0.13	-
29.6 grams of mass added to plate	120.0	0.05	-
37.1 grams of mass added to plate	118.6	0.18	-
59.1 grams of mass added to plate	113.4	0.05	-
100 grams of mass added to plate	105.8	0.14	-

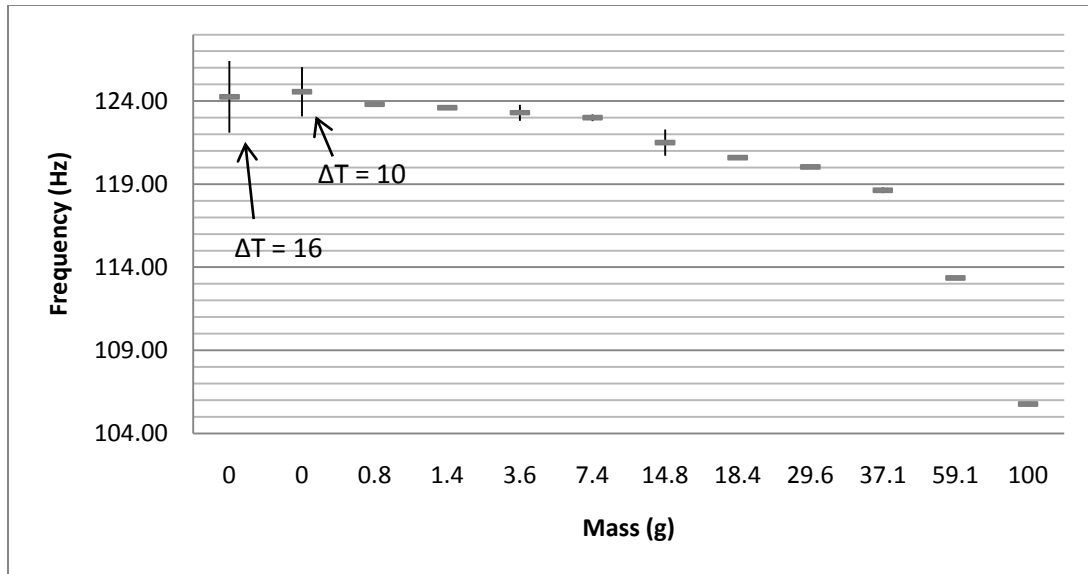


Figure 3.12: Frequency Ranges to One Standard Deviation for Each Mass Compared to Blank Plate Temperature Cycles

The first row of data in Table 3.7 combines all of the testing that was done once temperature began being recorded and it can be seen that throughout that time period, the temperature varied by 16 degrees. This was shown in an attempt to determine what range of fluctuation could be attributed to temperature fluctuation rather than to the added mass. In an attempt to reduce the influence of temperature fluctuation, a smaller window of time was analyzed which resulted in a smaller variance in temperature. For many days, testing was only done in the evenings from approximately 5 pm to 9 pm. This resulted in a temperature range of 10 degrees and as expected, a smaller standard deviation (Table 3.7).

Figure 3.12 can also be analyzed by investigating the results of testing when temperature fluctuation is eliminated. The standard deviations are sufficiently low that a mass of 7.4 grams can be distinguished from an added mass of only 0.8 grams (or no

added mass). When comparing the frequencies of the plate with masses added to the blank plate testing that saw a temperature range of 16 degrees, the first mass that falls outside of one standard deviation (and hence considered detectable) is 14.8 grams. Each subsequent mass also fell outside of the range of one standard deviation. When the blank plate saw a temperature variation of 10 degrees, the detectable mass did fall, but not as much as expected, to 7.4 grams. Each subsequent mass was also detectable for this case. This result can be compared to the first detectable mass of 5 grams from tests at location 1 where no temperature data was taken. Hence, stability or corresponding detection of temperature significantly improves detectability.

A satellite in orbit can typically expect to experience temperatures in the range of -130°C and 100°C with changes occurring in minutes (Larson and Wertz, 1991). Having seen what a temperature range of 16 degrees does to the modal behavior of an aluminum plate, one can expect to see a much wider range of results when dealing with a temperature range of over 200°C. There exists a thermal subsystem on the satellite which manages the temperature of the equipment by means of the physical arrangement of the equipment and using thermal insulation and coatings to balance heat from power dissipation, absorption from the Earth and Sun, and radiation to space (Larson and Wertz, 1991). Given all of this, it's evident that thermal effects will play a crucial role in any space structure health monitoring.

## Chapter 4

### SATELLITE TESTING

#### Testing on Satellite Panels

Vibration testing was done at the Air Force Research Lab Space Vehicles Directorate on two different setups: A couple of iso-grid satellite panels and a mock satellite.

#### PnP 2 Iso-Grid Satellite Panel

First, an accelerometer was placed on an aluminum satellite panel, called PnP 2, which was attached at a 90 degree angle to a larger satellite panel, called PnP 1. PnP 1 was clamped down to a large table in an attempt to steady the setup as much as possible. PnP 2 is an iso-grid aluminum alloy satellite panel that measures 0.5m x 1m and PnP 1 is an iso-grid aluminum alloy satellite panel that measures 1m x 1m. The mass of PnP 2 is roughly 7.80 kg and 17.42 for PnP 1. Figure 4.1 below shows a diagram of the setup.

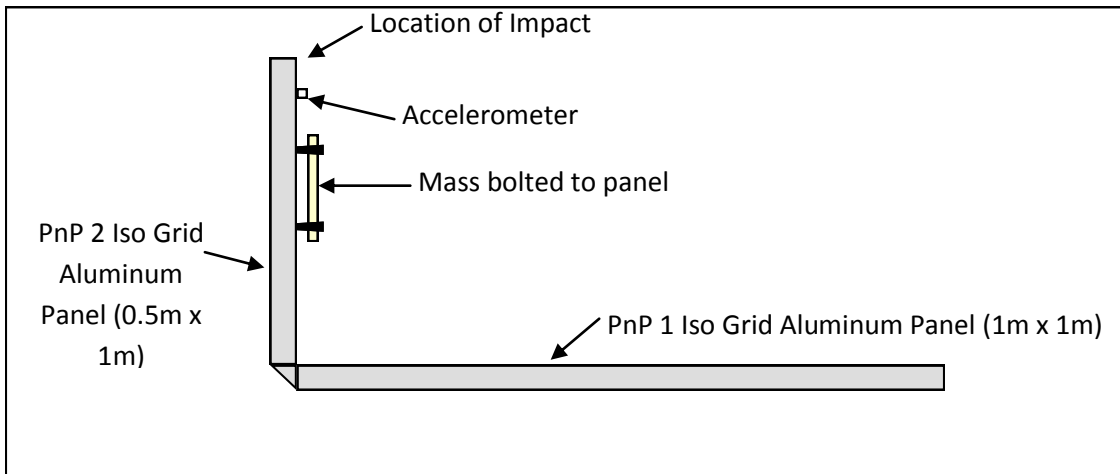


Figure 4.1: PnP 2 Test Panel Setup

With the larger panel lying down on the table, the smaller panel acted as a cantilever. The connection between the two panels consisted of 3 aluminum angles which were bolted to each panel. This connection did not allow for rotation or translation. The accelerometer was attached to the cantilever end of the smaller panel which was also the end that was impacted with the rubber mallet. As mentioned, the larger panel was bolted down to a large table to fix the entire setup. See Figures 4.2 and 4.3 showing photos of the setup.

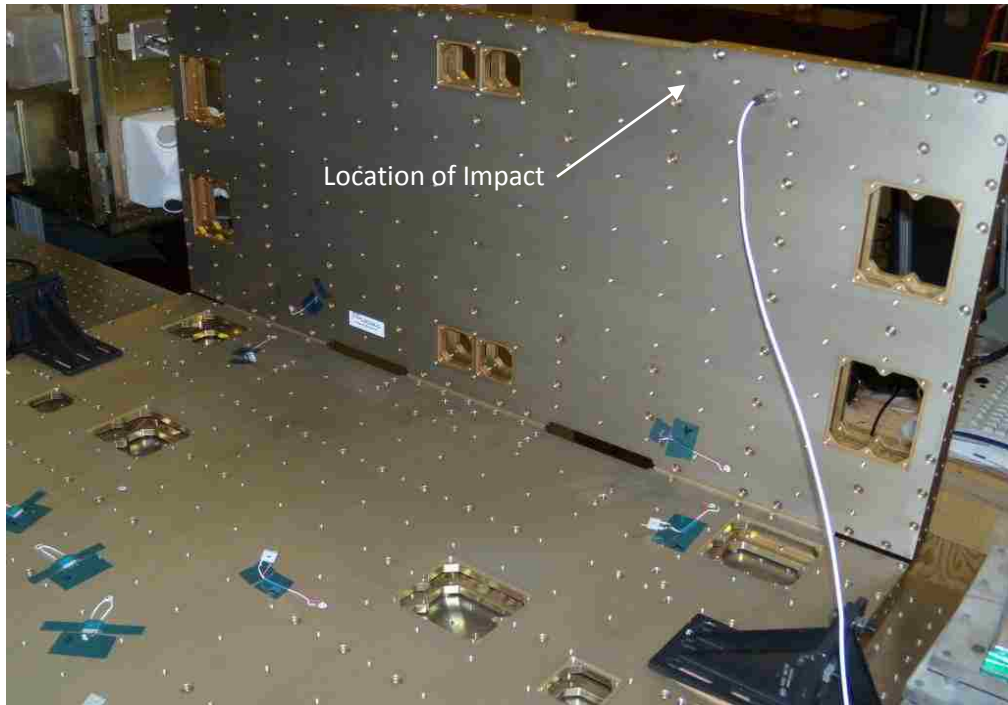
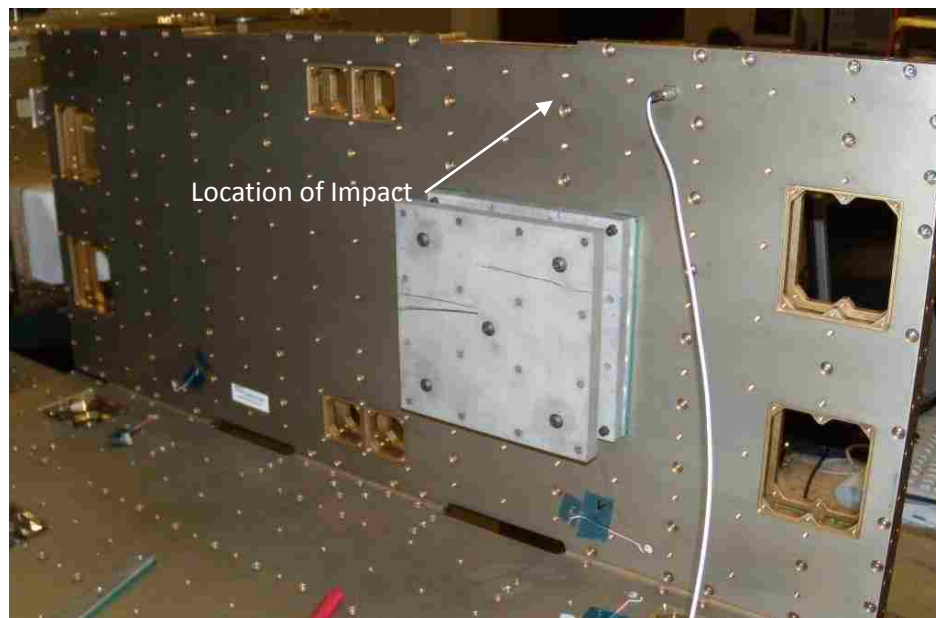


Figure 4.2: Photo of PnP 2 Setup Showing Accelerometer Location



Figure 4.3: Photo Showing How the Setup was Clamped to the Table

There were only a few different types and sizes of masses available for attaching to the satellite panel due to the bolt pattern on the panel. These masses can be seen in Figure 4.3 in the top right corner of the photo. Similar to the testing that was done on the aluminum plate setup, frequency testing of the satellite panel was performed with no mass present and then with increasing masses. The following photo shows the location that the masses were added.



**Figure 4.4: Photo of PnP 2 Setup Showing a Mass Bolted to the Plate**

Due to the testing being performed in a lab, the temperature, which was checked, remained constant throughout the entire testing process. Therefore, temperature data was not recorded with any of this testing. See results of testing on PnP 2 below in Table 4.1.

Table 4.1: Statistical Results of Testing on PnP 2

AFRL PnP 2 Iso Grid Panel		
Mass (g)	Average (Hz)	Std. Dev. (Hz)
0	48.5	0.22
30.5	48.5	0.05
54	48.5	0.06
108	48.4	0.05
162	48.2	0.07
216	47.9	0.05
246.5	47.8	0.06
2819	43.7	0.11
2849.5	43.6	0.04
5678	40.0	0.13

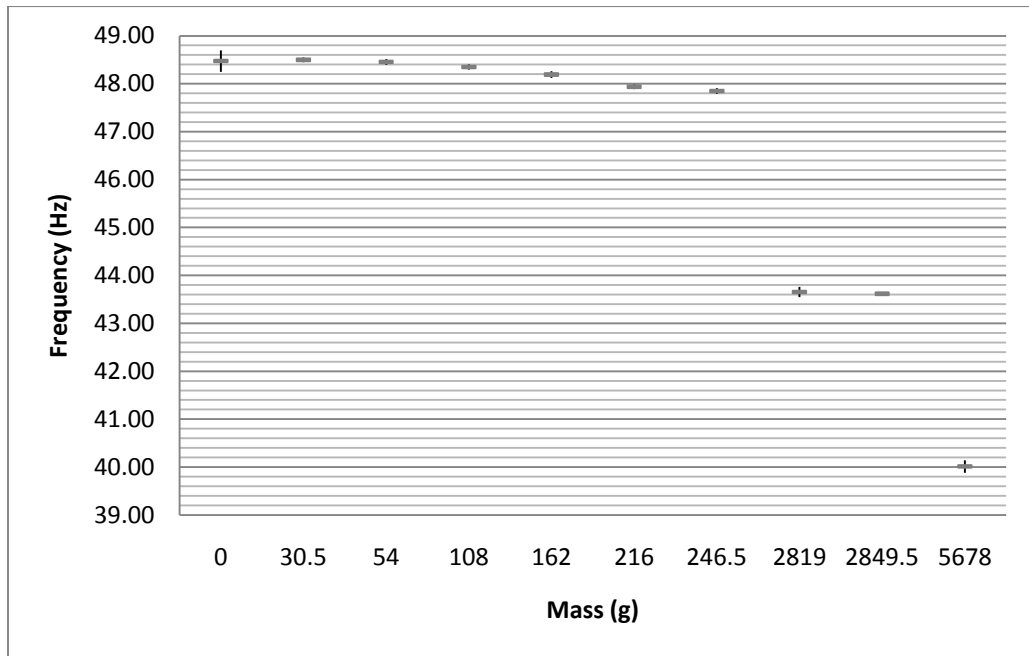


Figure 4.5: Frequency Ranges to One Standard Deviation for PnP 2 Testing

As can be seen from Table 4.1 and Figure 4.5 above, a 2819 gram mass or greater added to the panel has a substantial effect on the natural frequency of the panel and would be easily detectable through this type of testing. A closer look at the data up to

246.5 grams (Figure 4.6) shows that the 162, 216 and 246.5 gram masses fell well outside the range of one standard deviation of the mean for the blank panel and would be detectable in this scenario.

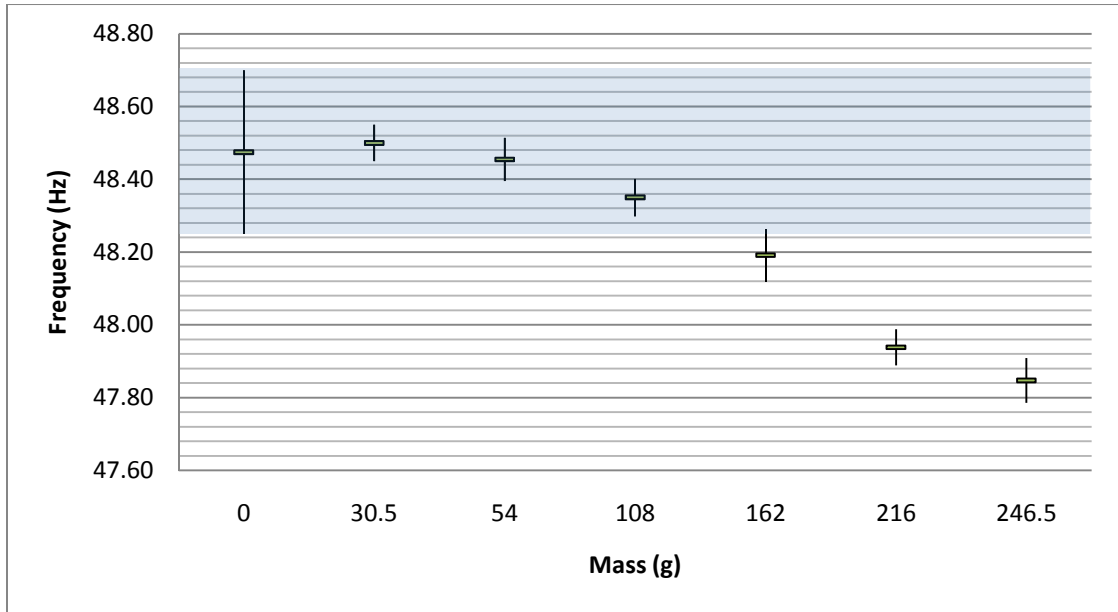


Figure 4.6: Frequency Ranges to One Standard Deviation for PnP 2 Testing from 0-246.5 grams

We can also see that 162 grams and greater is distinguishable from the baseline condition per the evaluation criteria. One could argue that the shift in the mean frequency between the baseline condition and 108 grams is sufficient enough to allow a mass of 108 grams to be detectable.

### **Mock Satellite Testing**

The second test setup at the Air Force Research Laboratory Space Vehicles Directorate was a mock satellite. Six aluminum iso-grid satellite panels were erected in the shape of a cube and dummy payloads were added on each side. The connection

between each panel consisted of a hinge that effectively allows for rotation but not translation. The weight of the mock satellite was not measured but roughly calculated based on the known mass of the satellite panels PnP 1 and PnP 2, giving a mass of approximately 66 kg. The following figure shows the basic configuration.

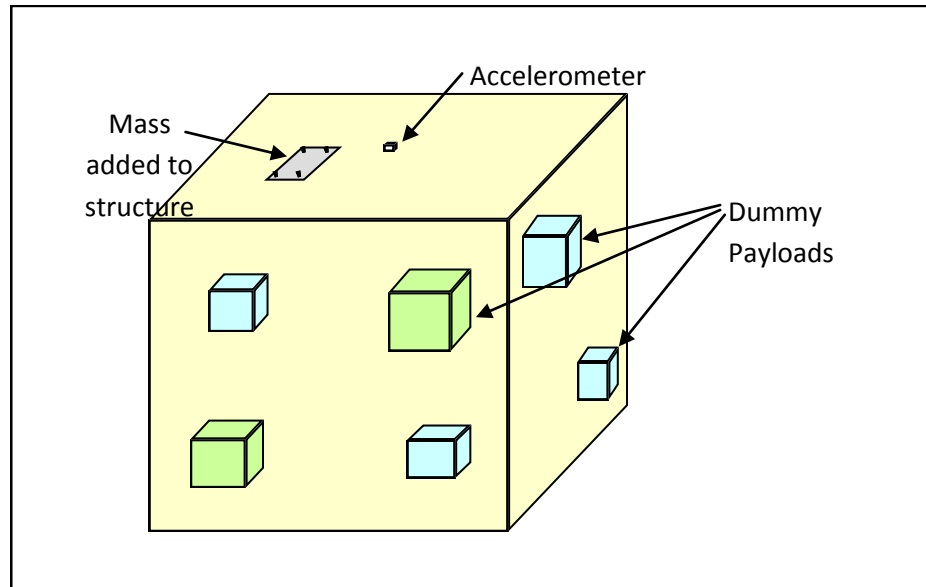


Figure 4.7: Diagram of Mock Satellite Test Setup



Figure 4.8: Photo of Mock Satellite Test Setup with Mass Attached



Figure 4.9: Photo Showing Connection Between Panels on Mock Satellite

The mock satellite was the most practical application. However, it was also the set-up where the least amount of testing was done due to other constraints. The bolt

pattern on this mock satellite did not match the bolt pattern on the PnP 2 satellite panel or the bolt pattern for the available masses. Hence, there were only a few of the masses that were actually available to be attached to the top panel. Table 4.2 shows the results of the testing done on this structure.

**Table 4.2: Statistical Results for Mock Satellite Testing**

AFRL Mock Satellite		
Mass (g)	Average (Hz)	Std. Dev. (Hz)
0	43.0	0.44
108	43.1	0.24
2819	40.1	0.25
5678	38.6	0.22

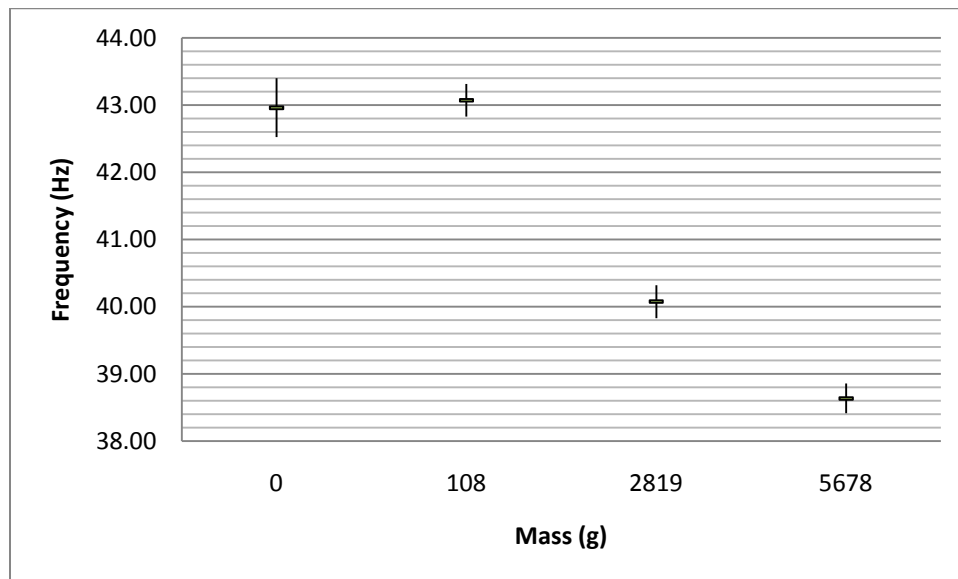


**Figure 4.10: Frequency Range to One Standard Deviation for Mock Satellite Testing**

Even though the connections between the panels on the mock satellite were hinges that allowed for rotation, the structure as a whole was extremely rigid and it was conjectured before testing began that the natural frequency of the panel may not be

distinguishable from that of the structure. Fortunately, a natural frequency was seen and as seen from the results, the addition of a mass did have affect on the vibration of the structure. Unfortunately, there weren't masses available to experiment with between 108 grams and 2819 grams. From the graph, it can be seen that the frequencies obtained with the presence of the 108 grams of mass fall directly with the range of frequencies obtained with no mass present and therefore would not be detectable. On the other hand, results obtained with the presence of 2819 grams of mass are well outside of the range and thus easily detectable. Even though the size of the detectable mass on the mock satellite couldn't be narrowed down any further, the overall goal of determining whether or not the addition of a mass could be detected through vibration-based monitoring was successful.

## Chapter 5

### CONCLUSIONS

#### Conclusion

The three test setups (aluminum plate, PnP 2 and the mock satellite) each provided their own unique opportunity to determine solutions from what could arise as potential problems experienced while trying to do vibration-based testing on an orbiting satellite. The aluminum plate provided the opportunity for large variety of testing and also exposed the problem created by temperature fluctuations. The iso-grid panel PnP 2 enabled testing to be done on an actual satellite panel and the mock satellite allowed for testing on a large-scale model of a satellite.

It was observed that the simply-supported case is difficult to emulate in the laboratory due to the bolted connection. Other than the simply-supported case, the results obtained by the computer model are similar to the experimental results and the analytical solutions. Also explained was the difference in the solutions for the 2<sup>nd</sup> and higher modes for analytical solutions versus the computer solutions; only the 1<sup>st</sup> mode was used in subsequent analysis and interpretation – Providing a rigid support to the test apparatus was also important as evident from conducting the tests on the floor vs. on a table. Ultimately, the objective of determining the accuracy of a finite element program to model the experimental data upon adding masses to the plate was successful.

Compared to a mass of 740 grams for the aluminum plate, added mass as small as 14.8 grams (approximately 2.0% of the weight of the plate) was detectable in spite of temperature fluctuations. The detectability improved to 7.4 grams when temperature fluctuation was eliminated. Based on these results, it becomes clear that more focus needs to be directed towards reduction or measurement of the thermal effects on the material behavior. This can lead to significant improvement in detectability. The threshold of detectability on an actual satellite panel (PnP 2) was established through testing.

As mentioned, 100 grams was the upper limit of mass detection on the aluminum plate due to anything larger damping the vibration too quickly to observe a natural frequency. This type of limit was not seen with the testing done on the Air Force Research Laboratory Space Vehicles Directorate panels and satellite but one could hypothesize that the upper limit may exist around 15-20% of the total mass of the structure. Similar to the aluminum test plate, the minimum mass detectability on the satellite panels and the mock satellite is a very small percentage of the total mass of the structure.

Finite element models of the iso-grid panels and the mock satellite were not within the scope of this research. However, results from the model of the aluminum plate give confidence in the reliability of SAP2000 to accurately model the modal behavior of a structure while adding masses.

Even though the fundamental frequencies of spacecrafts are usually known by the launch vehicle contractor prior to launching the craft into orbit (Larson and Wertz, 1999), they may change slightly once in orbit. Determining the fundamental frequency of the spacecraft once it goes into orbit becomes important because a baseline needs to be identified. See Appendix B for lists of different satellites and their fundamental frequencies.

### **Recommendations for Future Work**

As mentioned, temperature effects on frequency response are an important factor that must always be considered when doing vibration-based testing. This research incorporated temperature data into the behavior of the aluminum plate but only for a limited range. For any application on space structures, temperature must be an integral part of the analysis and must incorporate a wide range of temperatures and associated material behaviors. Taking into account the spacecraft's thermal subsystem would also be helpful in determining the typical temperature ranges a spacecraft should expect to experience.

Changes in stiffness, whether local or distributed, lead to changes in the natural frequencies of a vibrating system (Adams et al., 1978). Understanding that, there is a concern of being able to make a distinction between an added mass and damage to a structure when using FRF's as a method of monitoring. One might expect damage and a loss of mass to be the same thing and that a loss of mass might have the opposite effect of an added mass. It was seen that an added mass would cause the vibration of the

structure to dampen out much quicker; therefore, a loss of mass may have the effect of reduced stiffness and an increase in natural frequency of the structure. Either way, the difference in the two scenarios presents an interesting focal point for future research.

By far the most interesting potential topic for future work involves methods of testing satellite structures. Obviously, remote wireless monitoring is the only option when dealing with a space structure. Wireless monitoring of a structure is nothing new but what specifically becomes challenging with vibration-based monitoring is how to excite the structure. Peteers et al. (2001) looked at different excitation sources on vibration-based structural health monitoring of bridge, as well as temperature effects. He investigated the difference in using normal traffic flow, mass shakers, a drop weight and ambient sources such as wind or earthquakes. When operating in space, excitation of a structure becomes much more complex. There are so-called natural sources of excitation such as impacts with other objects. A satellite can be bombarded with the surrounding atmosphere at orbital velocities on the order of 8 km/s (Larson and Wertz, 1999). The only other apparent option would be to generate the excitation somehow. Spacecrafts have thrusters and various methods of propulsion for orientation purposes that could be viable sources of excitation. There has also been research done into the use of Piezoceramic (PZT) actuator-sensor as both an excitation and data gathering sensor (Ritdumrongkul et al. (2003, 2004) and Tanner et al. (2003)).

## Appendix A: Material Properties for the Aluminum Test Plate

<b>Material</b>	<b><math>\rho</math></b>	<b><math>F_{tu}</math></b>	<b><math>F_{cy}</math></b>	<b>E</b>	<b>e</b>	<b><math>\alpha</math></b>
<b>Alloy</b>	<b>(lb/in<sup>3</sup>)</b>	<b>(10<sup>3</sup> lb/in<sup>2</sup>)</b>	<b>(10<sup>3</sup> lb/in<sup>2</sup>)</b>	<b>(10<sup>6</sup> lb/in<sup>2</sup>)</b>	<b>(%)</b>	<b>(10<sup>-6</sup>/°F)</b>
6061-T6 Aluminum	0.098	42	35	9.9	10	12.7

$\rho$  = density

$F_{tu}$  = Allowable Tensile Ultimate Stress

$F_{cy}$  = Allowable Compressive Yield Stress

E = Modulus of Elasticity

e = Elongation

$\alpha$  = Coefficient of Thermal Expansion

## **Appendix B: Fundamental Frequencies for Various Satellites**

From Larson and Wertz (1999):

<b>Launch System</b>	<b>Fundamental Frequency (Hz)</b>	
	<b>Axial</b>	<b>Lateral</b>
Atlas II, IIA, IIAS	15	10
Ariane 4	31	10
Delta 6925/7925	35	15
Long March 2E	26	10
Pegasus, XL	18	18
Proton	30	15
Space Shuttle	13	13
Titan II	24	10

## References

Wu Z., Qing X., P., Chang F., (2009), "Damage Detection for Composite Laminate Plates with A Distributed Hybrid PZT/FBG Sensor Network. *Journal of Intelligent Material Systems & Structures*, Vol. 20 Issue 9, p1069-1077

Qing, X. P.; Beard, S. J.; Kumar A., Teng K. O., Chang F. (2007), "Built-in Sensor Network for Structural Health Monitoring of Composite Structure", *Journal of Intelligent Material Systems & Structures*, Vol. 18 Issue 1, p39-49.

Tanner, Neal A., Wait, Jeannette R., Farrar, Charles R., and Sohn, Hoon, (2003) "Structural Health Monitoring Using Modular Wireless Sensors." *Journal of Intelligent Material Systems and Structures*, 14, 43-56.

Wertz, James R. and Larson, Wiley J. (1991). *Space Mission Analysis and Design*, 3rd Edition, Microcosm Press, El Segundo, CA.

Adams R. D., Cawley P., Pye C. J. and Stone B. J. (1978). A vibration technique for non-destructively assessing the integrity of structures. *Journal of Mechanical Engineering Science*. 20, 93-100.

Zang, C., Friswell, M. I., and Imregun, M. (2007). "Structural Health Monitoring and Damage Assessment Using Frequency Response Correlation Criteria." *Journal of Engineering Mechanics*, 133(9), 981-993.

Shi, Z. Y., Law, S. S., and Zhang, L. M. (2000). "Damage localization by directly using incomplete mode shapes." *Journal of Engineering Mechanics*, 126(6), 656-660.

Sampaio, R. P. C., Maia, N. M. M., Silva, J. M. M., and Almas, E. A. M. (2003). "Damage Detection in Structures: From Mode Shape to Frequency Response Function Methods." *Mechanical Systems and Signal Processing*, 17(3), 489–498.

Peeters, Bart, Maeck, Johan, De Roeck, Guido, (2001). "Vibration-Based Damage Detection in Civil Engineering: Excitation Sources and Temperature Effects." *Smart Materials and Structures*, 10(3), 518-527.

Chatterjee, A. (2010). "Structural Damage Assessment in a Cantilever Beam with a Breathing Crack Using Higher Order Frequency Response Functions." *Journal of Sound and Vibration*, 329(16), 3325-3334.

Moreno, D., Barrientos, B., Perez-Lopez, C., Mendoza Santoyo, F., (2005). "Modal Vibration Analysis of a Metal Plate by Using a Laser Vibrometer and the POD Method." *Journal of Optics A: Pure and Applied Optics*, 7, S356-S363.

Botta, F., Cerri, G., (2007). "Shock Response Spectrum in Plates Under Impulse Loads." *Journal of Sound and Vibration*, 308, 563-578.

Chopra, Anil K. (2007). *Dynamics of Structures: Theory and Applications to Earthquake Engineering*, 3<sup>rd</sup> Edition, Pearson Prentice Hall, Upper Saddle River, NJ.

Ritdumrongkul, S., Fujino, Y. (2006). "Identification of the Location and Level of Damage in Multiple-Bolted-Joint Structures by PZT Actuator-Sensors." *Journal of Structural Engineering*, 132(2), 304-311.

Ritdumrongkul, S., Masato, A., Fujino, Y. Miyashita, T. (2004). "Quantitative Health Monitoring of Bolted Joints Using a Piezoceramic Actuator-Sensor." *Smart Materials and Structures*, 13, 20-29.

Lee, U., Shin, J. (2002). "A Frequency-Domain Method of Structural Damage Identification Formulated from the Dynamic Stiffness Equation of Motion." *Journal of Sound and Vibration*, 257(4), 615-634.